Construction and application of a solar radiation environment model in Chinese solar greenhouse

Fen He[1,2], Xiaoming Ding[1,2], Guanshan Zhang[3], Binbin Gong[4], Fei Qi[1,2*]

(1. *Academy of Agricultural Planning and Engineering, Ministry of Agriculture and Rural Affairs, Beijing 100125, China*;
2. *Key Laboratory of Farm Building in Structure and Intelligent Construction, Ministry of Agriculture and Rural Affairs, Beijing 100125, China*;
3. *College of Mechanical and Electronic Engineering, Shandong Agricultural University, Tai'an 271018, Shandong, China*;
4. *College of Horticulutre, Hebei Agricultural University, Baoding 071001, Hebei, China*)

Abstract: In order to quantitatively analyze the light radiation environment inside Chinese solar greenhouse (CSG) and select reasonable building design parameters, a CSG solar radiation environment model reflecting various factors such as geographical location, outside solar radiation, orientation and building parameters, front roof shape, and covering materials was studied. The model considered the impact of both cloudy and sunny weather conditions on the inside solar radiation environment, and established a simulation calculation method for inside direct radiation and scattered radiation. When calculating solar scattered radiation, the ground reflected radiation and atmospheric longwave radiation was considered. When calculating the transmittance of covering material, a structural shading loss and dust film model was introduced to calculate its impacts on the transmittance. The model was validated experimentally in a CSG at Yongqing in Hebei Province, China. The results showed that the model can effectively simulate the solar radiation of various points such as the ground and wall in the greenhouse at any time, with an average relative error of 8.19% between the simulated and measured values. Based on the established model, the impact of the geographical location, azimuth angle, and building parameters of CSG on inside solar radiation were analyzed. The research results can provide theoretical references and relevant data for the wall and soil heat storage, crop planting, and energy balance of enclosure structures in CSG.

Keywords: CSG, light radiation environment, solar radiation model, geographical location, azimuth angle, building parameter
DOI: 10.25165/j.ijabe.20251805.9454

Citation: He F, Ding X M, Zhang G S, Gong B B, Qi F. Construction and application of a solar radiation environment model in Chinese solar greenhouse. Int J Agric & Biol Eng, 2025; 18(5): 69–75.

1 Introduction

In the past forty years, the rapid development of CSG has played an important role in increasing farmers' income and ensuring vegetable supply; meanwhile, it also has become one of the most profitable agricultural industries[1]. At present, the research on CSG mainly focuses on building parameters optimization[2-5], thermal environment models[6-8], heating technology[9-11], control systems[12-14], and others. Light radiation environment is one of the important factors in CSG, and it is not only the fundamental prerequisite for the plant photosynthesis[15,16], but also one of the necessary conditions for CSG overwintering production. Therefore, it is necessary to consider obtaining maximum solar radiation in CSG design. Compared with the outdoor environment, CSG has characteristics such as reduced, uneven, and changes of solar radiation. The solar radiation conditions inside a CSG depend on various factors such as geographical location, outside solar radiation, orientation and building parameters, roof shape and covering materials, condensation amount, etc.[17,18]. The inside solar radiation not only forms a complex pattern and spatial distribution, but also constantly changes with seasons and time. Testing of different regions and types of CSG is the most direct and effective method to obtain the distribution of light radiation environment[19]. There are significant spatial differences in the distribution of solar radiation in CSG. Not only does direct solar radiation affect crops, but the distribution of scattered solar radiation also affects crop photosynthesis and yield. The difference of solar radiation intensity in different parts is the main reason for the air temperature difference in the greenhouse, and it is the main reason for inconsistent crop growth. Whether it is sunny or cloudy, the solar radiation gradually decreases from the south edge of the CSG to the back wall in the north-south horizontal direction, with the lowest near the back wall[20]. In the east-west direction, due to the influence of the east and west gables, in addition to forming two triangular weak light zones at the east and west ends in the morning and evening, the distribution of solar radiation intensity in the east-west direction is relatively uniform before and after noon. There is a significant correlation between the total solar radiation inside the greenhouse and the total outside solar radiation under different weather conditions in each season, as well as between the total solar radiation inside the greenhouse and time.

For the already built CSG, direct testing can grasp temperature, solar radiation, humidity, and other factors. For greenhouses that are still in the design stage, the method is establishing models of inside solar radiation environment. By simulating the inside solar radiation

Received date: 2024-10-23 **Accepted date:** 2025-03-04
Biographies: **Fen He**, PhD, research interests: greenhouse environment engineering, Email: hefen_2005@163.com; **Xiaoming Ding**, MS, research interests: protected cultivation, Email: 32105255@qq.com; **Guanshan Zhang**, PhD, research interests: greenhouse environment engineering, Email: zgsh9919@sdau.edu.cn; **Binbin Gong**, MS, research interest: greenhouse environment engineering, Email: yygbb@hebau.edu.cn.
***Corresponding author: Fei Qi**, Professor, research interests: agricultural engineering. Academy of Agricultural Planning and Engineering, Ministry of Agriculture and Rural Affairs, Beijing 100125, China. Tel: +86-13901216776, Email: qf2008@188.com.

environment under different conditions, building schemes and parameters, a reasonable design plan can be determined based on scientific evaluation. This is a feasible way to achieve a good inside solar radiation environment for the designed CSG. Cao et al.[21] constructed a direct solar radiation simulation model, compiled a computer program, and analyzed the instantaneous and cumulative distribution of direct solar radiation on the ground, back wall, and back roof to optimize lighting surface. However, this model only considered direct solar radiation simulation and did not consider the reflected and scattered parts. Chen et al.[22] explored the impact of gable walls on solar radiation in greenhouse and used the cloud cover coefficient method to calculate the solar radiation on the ground inside and outside CSG under different cloud cover weather conditions. Xu et al.[23] established a solar radiation model for a sunny (cloudless) CSG based on meteorological data, the motion laws of the earth and the sun, and the relationship between solar radiation and the incidence angle of the front roof of the greenhouse. Ma et al.[24] established a relatively comprehensive CSG solar radiation model, but it was not verified by actual data. Zhang et al. [25] established a mathematical model to evaluate the light radiation environment of CSG, which took into account shape parameters, material optical properties, and inside solar radiation evolution. Huang et al.[26] proposed an improved mathematical model for calculating the total transmitted solar radiation captured by the surface of a CSG. The model uses the MATLAB platform to calculate the total solar radiation and considers the reflected radiation from the outdoor ground. Chen et al.[27] constructed a mathematical model applied for the first time to analyze and compare the amount of captured global solar radiation in various greenhouse shapes and orientations in southern China. Pieters et al.[28] used a semi one-dimensional climate model to investigate the relative importance of the constructional parameters that influence the solar energy collecting efficiency of greenhouses under Western European conditions.

The propagation law of solar radiation in greenhouse is complex, and there are many influencing factors. The current research provides valuable reference results for the in-depth study of the light radiation environment in CSG. However, it is difficult to establish a universal and comprehensive model that can describe the distribution and changes of direct and scattered solar radiation in a greenhouse under any weather condition, and this requires a large amount of data calculation and analysis. Currently, research mainly focuses on theoretical model simulation and a small amount of test data applied to model validation, and a large number of models are difficult for actual greenhouse engineering design and scheme optimization.

In this study, a CSG solar radiation environment model was constructed that reflects various factors such as geographical location, outdoor solar radiation, greenhouse orientation and building parameters, roof shape, and covering materials, and the experimental verification on the model was conducted. Based on the established model, the impact of variable building parameters on inside solar radiation was analyzed in the five typical cities of Beijing, Shenyang, Xi'an, Lanzhou, and Xining at different azimuth angles and under the most unfavorable lighting conditions on the winter solstice.

2 Materials and methods

2.1 Outside solar radiation from any orientation plane

Solar radiation from any orientation plane outside on a sunny day I_{sunny} is as follows:

$$I_{\text{sunny}} = I_{\text{D}\theta} + I_{\text{S}\theta} \tag{1}$$

where, $I_{\text{D}\theta}$ and $I_{\text{S}\theta}$ is direct and scattered solar radiation from any orientation plane outside on a sunny day, W/m^2.

At a specified time on a sunny day, the direct solar radiation obtained on any plane is related to the incident angle i of sunlight on that plane. If the inclination angle of calculated plane is θ, the intensity of direct solar radiation received is as follows[29]:

$$I_{D\theta} = I_0 \cdot p^m \cdot \cos i \tag{2}$$

$$I_0 = 0.0015x^6 - 0.0608x^5 + 0.8839x^4 - 5.284x^3 + 11.58x^2 - 20.099x + 1418 \tag{3}$$

$$\begin{cases} m = \dfrac{1}{\sin h}, & (h \geq 30^\circ) \\ m = \sqrt{1229 + (614\sin h)^2} - 614\sin h, & (h < 30^\circ) \end{cases} \tag{4}$$

$$\begin{cases} p = 0.0021x^2 - 0.0254x + 0.7005 (25^\circ\text{N}) \\ p = 0.0038x^2 - 0.0471x + 0.7707 (30^\circ\text{N}) \\ p = 0.0038x^2 - 0.0459x + 0.7691 (35^\circ\text{N}) \\ p = 0.0033x^2 - 0.0409x + 0.772 (40^\circ\text{N}) \\ p = 0.0039x^2 - 0.0481x + 0.787 (45^\circ\text{N}) \end{cases} \tag{5}$$

where, I_0 is the solar radiation constant, W/m^2; p is the atmospheric transparency; m is the atmospheric quality; x is the months of the year, ranging from 1 to 12; h is the solar altitude angle, (°).

The solar altitude angle can be calculated using the following equations:

$$\sin h = \cos\varphi \cdot \cos\delta \cdot \cos\omega + \sin\varphi \cdot \sin\delta \tag{6}$$

$$\delta = 23.45\cos\left(360\frac{n-172}{365}\right) \tag{7}$$

$$\omega = 15\left[\left(T_0 - \frac{120-\lambda}{15}\right) - 12\right] \tag{8}$$

where, φ is the location latitude, (°); δ is the declination angle, (°); ω is the hour angle, (°); n is the number of days calculated from January 1st; T_0 is the Beijing time, which is 0-24 h; λ is the location longitude, (°).

The scattered radiation received by any plane from air includes three terms, and it is as follows:

$$I_{\text{S}\theta} = I_{d\theta} + I_{\text{R}\theta} + I_B \tag{9}$$

where, $I_{d\theta}$ is the sky scattered radiation, W/m^2; $I_{\text{R}\theta}$ is the ground reflected radiation, W/m^2; I_B is the atmospheric longwave radiation, W/m^2.

$$I_{d\theta} = \frac{(1-p^m)\cdot I_0}{2(1-1.4\ln p)} \cdot \sin h \cdot \cos^2\frac{\theta}{2} \tag{10}$$

$$I_{\text{R}\theta} = \rho_G \cdot \left(I_0 \cdot p^m \cdot \sin h + \frac{(1-p^m)\cdot I_0}{2(1-1.4\ln p)}\right)\left(1-\cos^2\frac{\theta}{2}\right) \tag{11}$$

where, ρ_G is the average reflectance of ground which is 0.2.

$$I_B = 5.67\left(\frac{T_a}{100}\right)^4 (0.51 + 0.208\sqrt{e_a}) \tag{12}$$

$$e_a = \text{RH} \cdot e_s \tag{13}$$

where, T_a is the outside air temperature, °C; e_a is the air partial pressure of water vapor, Pa; e_s is the air saturated water vapor pressure, Pa; RH is the outside air relative humidity, %RH.

When T_a>273.15K, e_s can be calculated as follows[30]:

$$\ln e_s = (-7.902\,98)\left(\frac{373.16}{T_a}-1\right)+5.028\,08\ln\left(\frac{373.16}{T_a}\right)-(1.3816\times10^{-7})\left[10^{11.344\left(1-\frac{T_a}{373.16}\right)}-1\right]+(8.1328\times10^{-3})\left[10^{-3.491\,49\left(\frac{373.16}{T_a}-1\right)}-1\right]+\ln(1013.246) \quad (14)$$

When $T_a < 273.15K$, e_s is as follow.

$$\ln e_s = (-9.097\,18)\left(\frac{273.16}{T_a}-1\right)-3.566\,54\ln\left(\frac{273.16}{T_a}\right)+0.876\,793\left(1-\frac{T_a}{273.16}\right)+\ln(6.1071) \quad (15)$$

The total solar radiation on cloudy days I_{Cloudy} is mainly related to the amounts of clouds CC in the sky. When $CC \leq 2$, it is sunny weather, and the total solar radiation on a sunny day can represent the total solar radiation. When $2<CC<8$, it is common weather, and it may be sunny or cloudy. When $8 \leq CC \leq 10$, it is mostly cloudy. At present, the cloud cover coefficient method is used to calculate solar radiation on cloudy days[24]:

$$I_{\text{Cloudy}} = \text{CCF}\cdot I_{\text{Sunny}} \quad (16)$$

where, CCF is the cloud cover coefficient, which is as follows:

$$\begin{cases}\text{CCF}=1.06+0.012CC-0.0084CC^2 & \text{(March to May)}\\ \text{CCF}=0.96+0.033CC-0.0106CC^2 & \text{(June to August)}\\ \text{CCF}=0.95+0.030CC-0.0108CC^2 & \text{(September to November)}\\ \text{CCF}=1.14+0.003CC-0.0082CC^2 & \text{(December to February)}\end{cases} \quad (17)$$

$$I'_{\text{D}\theta} = \left(1-\frac{CC}{10}\right)\cdot I_{\text{D}\theta} \quad (18)$$

$$I'_{\text{S}\theta} = I_{\text{Cloudy}} - I'_{\text{D}\theta} \quad (19)$$

where, $I'_{\text{D}\theta}$ and $I'_{\text{S}\theta}$ is the direct and scattered solar radiation from any orientation plane outside on a cloudy day, W/m^2.

2.2 The transmittance of solar radiation on greenhouse covering materials

The transmittance of direct and scattered radiation is as follows[24]:

$$\tau_D = \tau_{Di}\cdot(1-r_1)\cdot(1-r_2)\cdot(1-r_3) \quad (20)$$

$$\tau_S = \tau_{\text{S0}}\cdot(1-r_1)\cdot(1-r_2)\cdot(1-r_3) \quad (21)$$

where, τ_D is the transmittance of direct radiation; τ_S is the transmittance of scattered radiation; τ_{Di} is the direct radiation transmittance of clean covering materials at an incident angle of i, $\tau_{Di} = (90-5^{(i-20)/25.06})$; τ_{S0} is the scattered radiation transmittance of clean covering materials, and the value is 70%-85%; r_1 is the structure shading loss rate, which is as follow[31]:

$$r_1 = \frac{\left[P_g\cdot\tan(90-h)+G_g\right]L_g\cdot\dfrac{M}{m_1}}{L\cdot M} \quad (22)$$

where, P_g is the thickness of skeleton, m; G_g is the width of the skeleton, m; L_g is the length of skeleton, m; M is the length of CSG, m; m_1 is the number of skeletons arranged per meter; r_2 is the transparency loss rate of covering materials due to aging, with values ranging from 0.15 to 0.3; r_3 is the transparency loss rate due to condensation of water droplets and dust. The specific calculation is as follows[32]:

$$r_3 = f(i,\rho_d) = 92.19+0.212i-2.676\rho_d-4.715\times10^{-3}i^2-6.501\times10^{-3}i\cdot\rho_d-1.726\times10^{-2}\rho_d^2 \quad (23)$$

$$\rho_d(k) = -4.6816k^3+20.883k^2-23.615k+9.2917 \quad (24)$$

where, ρ_d is the dust density, g/m^2; k is the absolute value of slope at any point on the front roof curve of CSG.

The relationship between the incident point of sunlight on the front roof and the calculated point on the ground inside the CSG is analyzed, as shown in Figure 1. The sunlight enters the greenhouse from point D and reaches point C on the ground. Given the coordinate position of inside ground point C, the coordinates of the corresponding point D can be determined by solving the roof curve Equations (25) and (26):

$$y_D = f(x_D) \quad (25)$$

$$tgh_{x,y} = \frac{y_D-y_C}{x_D-x_C} \quad (26)$$

where, x_D, y_D are the horizontal and vertical coordinates of point D, m; x_C, y_C are the horizontal and vertical coordinates of point C, m; $h_{x,y}$ is the angle between the projection of sunlight on the cross-section of a greenhouse and the horizontal plane, (°).

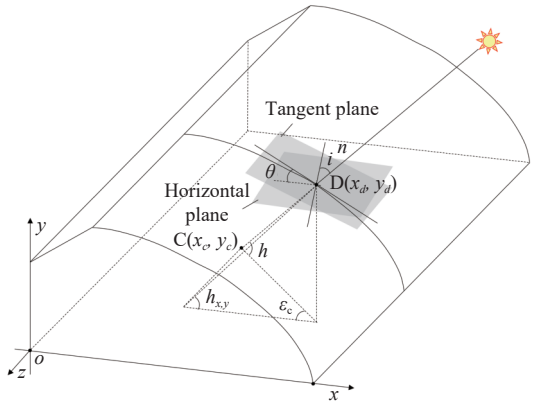

a. Three-dimensional diagram

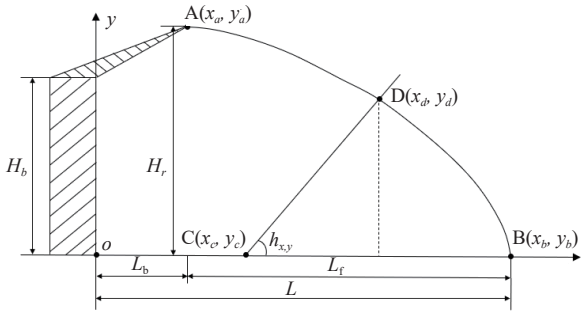

b. Cross section view

Figure 1 Analysis of the relationship between the sunlight incident point and inside points

$$tgh_{x,y} = \frac{tgh}{\cos\varepsilon_c} \quad (27)$$

$$\varepsilon_c = \alpha-\gamma_c \quad (28)$$

$$\cos i = \sin h\cdot\cos\theta+\cos h\cdot\sin\theta\cdot\cos\varepsilon_c \quad (29)$$

$$\sin\alpha = \frac{\cos\delta\cdot\sin\omega}{\cos h} \quad (30)$$

where, ε_c is the angle between the projection of the connecting line between the calculation point and the sun on the horizontal plane and the projection line of the tangent plane normal of the roof at the incident point on the horizontal plane, (°); α is the angle between

the projection of the line connecting the sun to a given point on the ground and the south direction, (°). When the sun is eastward, it is negative, and when it is westward, it is positive. γ_c is the intersection angle between the projection of the roof tangent plane normal at the incident point on the horizontal plane and the due south direction, (°). When the CSG is due south, then $\gamma_c = 0°$.

2.3 Solar radiation at any surface calculation point inside greenhouse

For any inside point C, the direct and scattered radiation of the sun I_{DC} and I_{SC} is related to the haze H of the covering material.

$$I_{DC} = \tau_D \cdot I_{D\theta} \cdot (1 - H) \tag{31}$$

$$I_{SC} = \left[1 - \frac{\arctan(H_r/(x_c - x_a))}{180}\right] \cdot \tau_S \cdot I_{S\theta} + H \cdot \tau_D \cdot I_{D\theta} \tag{32}$$

2.4 Experimental greenhouse description and data collection

The experiment was carried out in the CSG of Yongqing County, Hebei Province of China from October 2021 to April 2022 (39.42°N, 116.60°E, 11 m altitude). The CSG faces south, with a length of 60 m, a span of 10 m, and a ridge height of 5.32 m. The back wall was 4.35 m high and 950 mm thick. From inside to outside, it was 850 mm thick steel frame system prefabricated reinforced concrete slab fabricated wall and 100 mm thick extruded polystyrene board. The fabricated wall was a steel frame, the inner and outer layers were 80 mm thick precast concrete slabs, and the middle was 660 mm thick compacted soil, which needs to be compacted in several times. The gable was 370 mm thick shale brick with 100 mm thick extruded polystyrene board outside. The film of front roof was polyolefin film with high light transmittance, aging resistance, fog elimination, and good dripping performance, with a thickness of 0.12 mm. The front bottom of the greenhouse adopted electric film rolling ventilation, and the ridge adopted intelligent roof ventilation system to adjust the size of air outlet according to the inside air temperature feedback. The front roof was covered with composite insulation quilt, and the rolling time was 8:30-9:00 and 16:00-16:30. The air heating system was not installed in the greenhouse. Figure 2 is the schematic diagram of the experimental CSG.

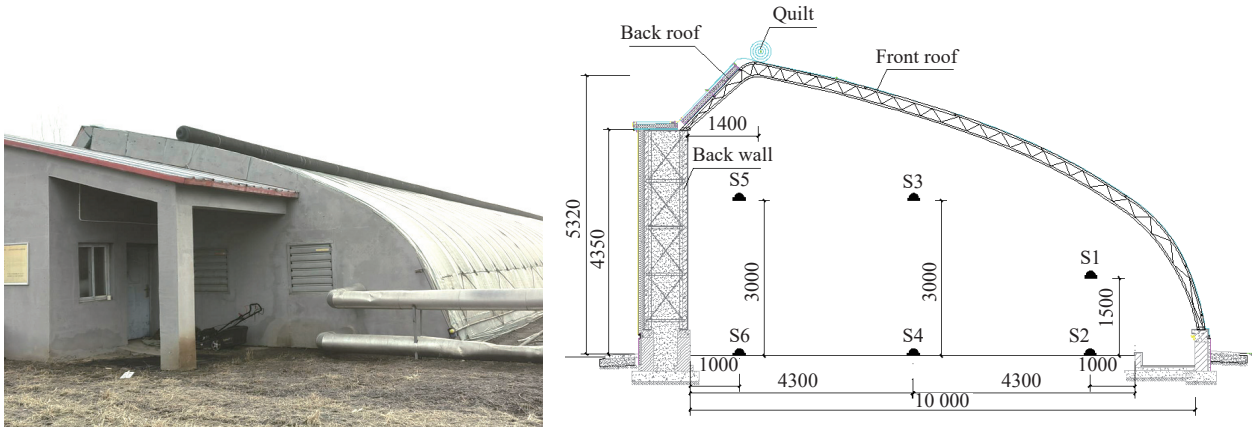

a. Physical picture b. Cross-sectional view of CSG and measuring points layout

Figure 2 Schematic diagram of experimental CSG

The test parameters were the inside and outside solar radiation. The outside solar radiation was measured using the meteorological station. The inside solar radiation was collected using total radiation sensor connected to data collector. The test parameters and equipment were listed in Table 1. Six solar radiation measurement points (S1, S2, S3, S4, S5, S6) were arranged in the central section of the CSG, as shown in Figure 2b. The collection time interval was 10 min.

Table 1 Test parameters and equipment

Test parameter	Instrument	Test range and accuracy	Producer
Inside total solar radiation	LI200X total radiation sensor	Spectral band: 400-1100 nm 0-1000 W·m^{-2}, ±30 W·m^{-2}	LI-COR Corporation, USA
Outside solar radiation	Vantage Pro2 outside meteorological station	Air temperature: –40°C-65°C Air relative humidity: 0-100% RH Solar radiation: 0-1800 W·m^{-2}	USA
-	CR1000 data collector	-	Campell Corporation, USA

3 Results and discussion

3.1 Distribution of light radiation environment

Taking the average of six measurement points as the inside solar radiation, Figure 3 shows the changes in total inside and outside solar radiation during the testing period. It can be seen that the change law of inside and outside solar radiation was consistent. Inside solar radiation was different from inside temperature, and there was no lag compared to outside solar radiation. Inside solar radiation is smaller than outside due to factors such as covering materials, structural components, and crops.

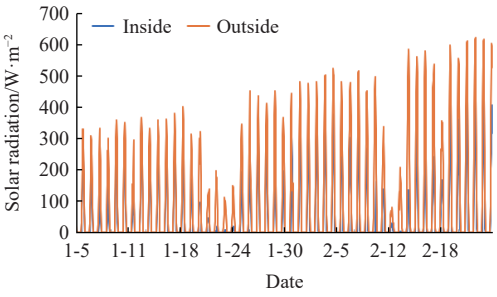

Figure 3 Total inside and outside solar radiation

The environmental changes inside CSG were analyzed under two typical weather conditions: 1) One day in a continuous sunny day (January 6, 2022); 2) A continuous cloudy and snowy day (January 21, 2022). Figure 4 shows inside solar radiation changes with outside solar radiation for both sunny and snowy days. After the insulation was rolled up from 8:00 to 8:30, the inside solar radiation gradually increased and reached its peak around 12:00. After the insulation was put down at 16:00, there was no solar

radiation inside. On cloudy and snowy days, the highest outside solar radiation value was 140 W/m^2, which was 160 W/m^2 lower than on sunny days. The maximum inside solar radiation was less than 60 W/m^2. It can be seen that under cloudy and snowy conditions, due to weak inside and outside solar radiation, the inside temperature was low, which could not meet the most suitable light and temperature environment required by crops, and was prone to adverse effects.

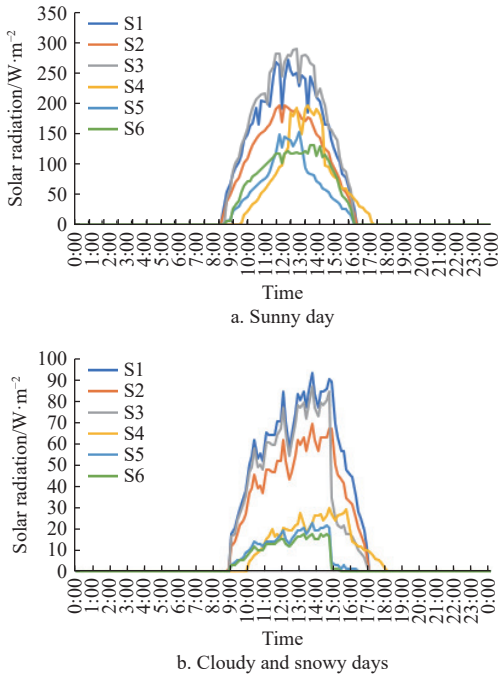

Figure 4 Daily change of CSG solar radiation

3.2 Simulation and analysis of light radiation environment

The outside meteorological conditions from February 13-19, 2022 were selected as input parameters of the solar radiation model. Figure 5 shows the measured and simulated values of the mean values of six measurement points.

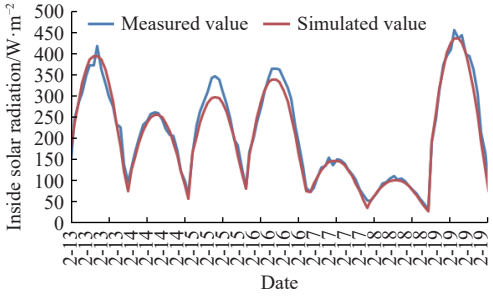

Figure 5 Simulated and measured value variation curve of CSG

Statistical analysis was conducted on the simulated relative error of points S1 to S6, as listed in Table 2. The average relative error of all measurement points was 8.19%, which showed that the simulated and measured values were in good agreement, and the model accuracy was high.

3.3 Influence of different factors on inside light radiation environment

3.3.1 Geographic location

The main areas for CSG in China are in North China, Northwest China, Northeast China, and other regions. Five typical cities were selected, including Beijing (39.93°N, 116.33°E), Shenyang (41.80°N, 123.43°E), Xi'an (34.27°N, 108.93°E), Lanzhou (36.058°N, 103.824°E), and Xining (36.56°N, 101.56°E), to simulate solar radiation in CSG on the winter solstice (December 22, 2022), as shown in Figure 6.

Table 2 Statistics of errors between measured and simulated values

Measure point	February 13th (Sunny)	February 14th (Cloudy)	February 15th (Cloudy)	February 16th (Sunny)	February 17th (Cloudy)	February 18th (Sunny)	February 19th (Sunny)
S1	10.6%	4.4%	8.1%	6.9%	9.5%	6.7%	10.2%
S2	6.9%	6.9%	9.6%	9.2%	9.8%	8%	9.9%
S3	7.9%	4.0%	8.2%	9.7%	10.4%	7.5%	10.5%
S4	6.5%	5.5%	7.3%	10.2%	9.3%	6.2%	10.3%
S5	8.5%	6.4%	8.6%	8.9%	10.7%	6.8%	9.5%
S6	7.3%	5.8%	6.8%	7.8%	10.2%	7.1%	9.4%
Average relative error	7.95%	5.50%	8.10%	8.78%	9.98%	7.05%	9.97%

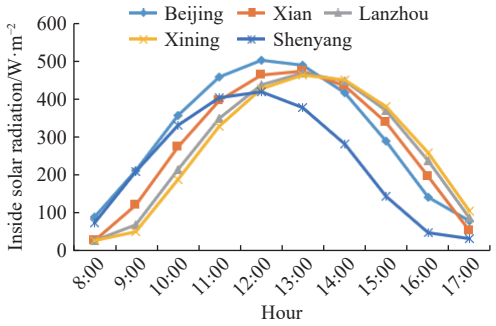

Figure 6 Simulation of solar radiation in typical urban CSG

3.3.2 Azimuth angle

Solar radiation in different directions of CSG was simulated in five cities, with settings of due south (azimuth angle is 0°), east 5°, east 10°, west 5°, and west 10°, as shown in Figure 7. The influence of changing azimuth angles on the simulated solar radiation values in five urban CSGs was consistent. When the CSG was west 10°, west 5°, due south, east 5°, and east 10°, the inside solar radiation reached its peak in sequence.

3.3.3 Building parameters

Taking the winter solstice in Beijing as an example, eight combinations of CSG building parameters (Table 3) were designed to simulate inside solar radiation. A1-A4 represented the combination of building parameters with variable ridge height, and B1-B4 represented the combination of building parameters with horizontal projection of back roof. The simulation results are shown in Figure 8. When the ridge height changed, there was a significant change in the daily variation of inside solar radiation. During the period from 9:00 to 16:00, inside solar radiation increased with the increase of ridge height. When the horizontal projection of back roof changed, the daily variation of inside solar radiation was not significant.

Table 3 Combination of building parameters

Type	Span/m	Ridge height/m	Height of back wall/m	Horizontal projection of back roof/m	The length of back roof/m
A1	10	5.72	4	1.3	2.16
A2	10	5.32	4	1.3	1.85
A3	10	4.92	4	1.3	1.59
A4	10	4.52	4	1.3	1.40
B1	10	5.32	4	0.9	1.60
B2	10	5.32	4	1.3	1.85
B3	10	5.32	4	1.7	2.15
B4	10	5.32	4	2.1	2.48

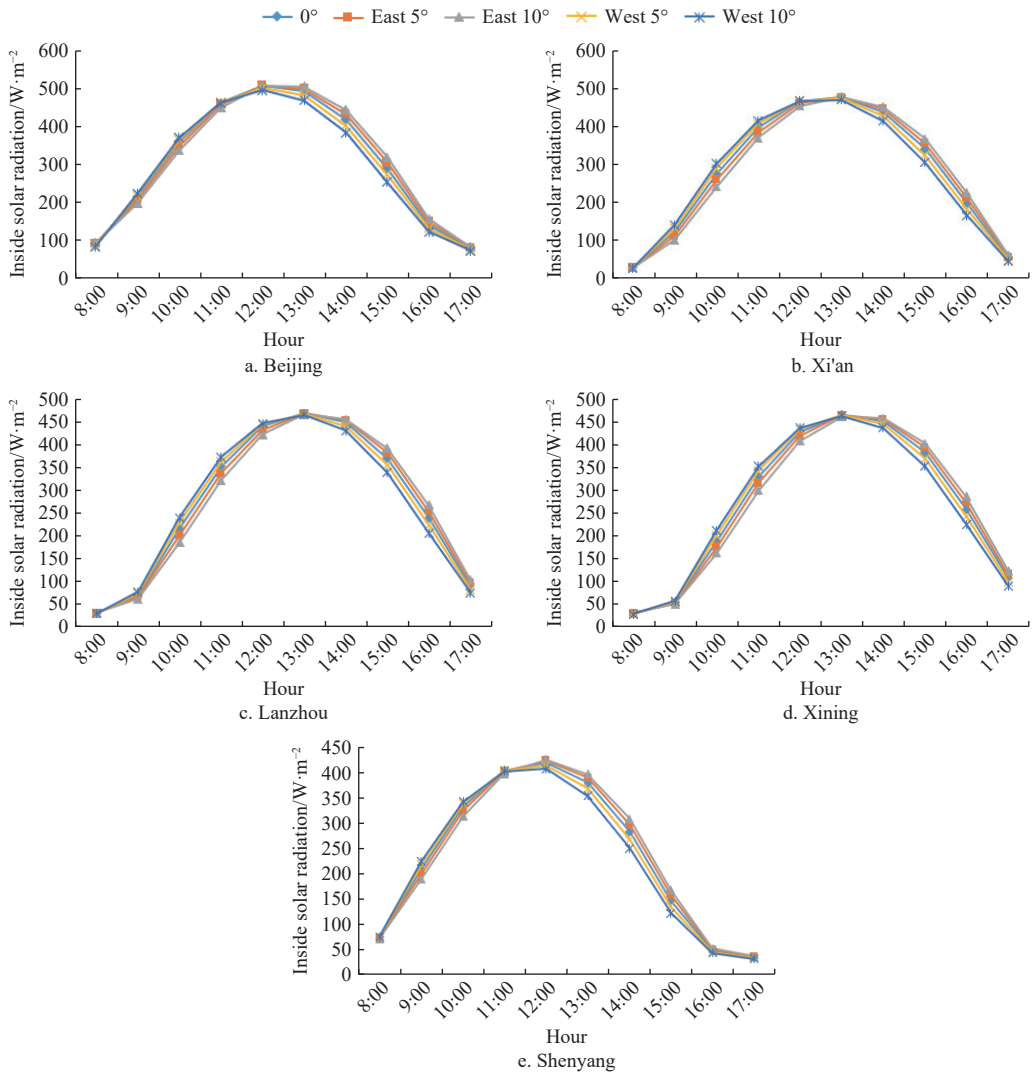

Figure 7 Simulation of solar radiation at different azimuth angles

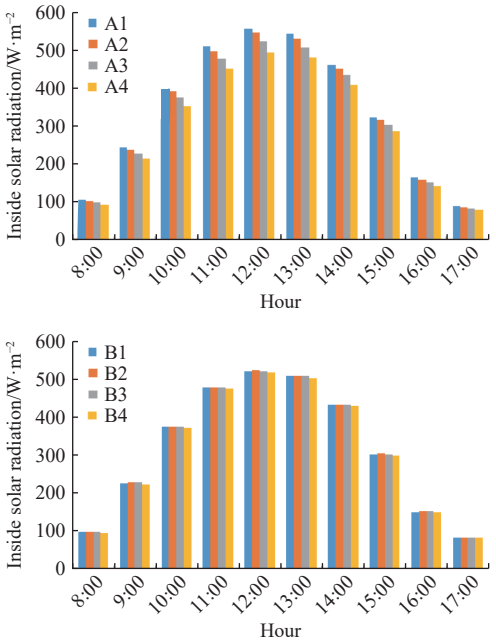

Figure 8 Simulation of solar radiation under different building parameters

4 Conclusions

A CSG solar radiation environment model reflecting various factors such as geographical location, outside solar radiation, greenhouse orientation and building parameters, front roof shape, and covering materials was constructed. The model was validated in a CSG at Yongqing in Hebei Province. The results showed that the model's average relative error was 8.19% between the simulated and measured values. Based on the model, the impact of the geographical location, azimuth angle, and building parameters of CSG on inside solar radiation was analyzed.

Acknowledgement

The authors would like to acknowledge the support provided by Agricultural Planning Talent Project of Academy of Agricultural Planning and Engineering, MARA (Grant No. QNYC-2024-10), Independent Research and Development Plan of Academy of Agricultural Planning and Engineering, MARA (Grant No. SH202402 and Grant No. SP202101), National Natural Science Foundation of China (Grant No. 32201657), and Shandong Natural Science Foundation Project (Grant No. ZR2021QF091).

[References]

[1] Xu D M, Li Y M, Zhang Y, Xu H, Li T L, Liu X G. Effects of orientation and structure on solar radiation interception in Chinese solar greenhouse. Plos One, 2020; 15(11): e0242002.

[2] Zhang R, Liu Y C, Zhu D L, Zhang X M, Ge M S, Cai Y H. Optimal design for solar greenhouses based on canopy height. Journal of Building Engineering, 2022; 53: 104473.

[3] Esmaeli H, Roshandel R. Optimal design for solar greenhouses based on climate conditions. Renewable Energy, 2020; 145: 1255–1265.
[4] Tong G H, Christopher D M, Zhang G Q. New insights on span selection for Chinese solar greenhouses using CFD analyses. Computers and Electronics in Agriculture, 2018; 149: 3–15.
[5] He F, Si C Q, Ding X M, Gao Z J, Gong B B, Qi F, et al. Optimization of Chinese solar greenhouse building parameters based on CFD simulation and entropy weight method. Int J Agric & Biol Eng, 2023; 16(6): 48–55.
[6] Mobtaker H G, Ajabshirchi Y, Ranjbar S F, Matloobi M. Simulation of thermal performance of solar greenhouse in north-west of Iran: An experimental validation. Renewable Energy, 2019; 135: 88–97.
[7] Dong S Y, Ahamed M S, Ma C W, Guo H Q. A time-dependent model for predicting thermal environment of mono-slope solar greenhouses in cold regions. Energies, 2021; 14(18): 5956.
[8] Tong G, Christopher D M, Li B. Numerical modelling of temperature variations in a Chinese solar greenhouse. Computers and Electronics in Agriculture, 2009; 68: 129–139.
[9] Cao K, Xu H J, Zhang R, Xu D W, Yan L L, Sun Y C, et al. Renewable and sustainable strategies for improving the thermal environment of Chinese solar greenhouses. Energy and Building, 2019; 202: 109414.
[10] Lu W, Zhang Y, Fang H, Ke X L, Yang Q C. Modelling and experimental verification of the thermal performance of an active solar heat storage-release system in a Chinese solar greenhouse. Biosystems Engineering, 2017; 160: 12–24.
[11] Sun W T, Wei X M, Zhou B C, Lu C G, Guo W Z. Greenhouse heating by energy transfer between greenhouses: System design and implementation. Applied Energy, 2022; 325: 119815.
[12] Wang Y G, Lu Y J, Xiao R M. Application of nonlinear adaptive control in temperature of Chinese solar greenhouses. Electronics, 2021; 10(13): 1582.
[13] Yu H H, Chen Y Y, Hassan S G, Li D L. Prediction of the temperature in a Chinese solar greenhouse based on LSSVM optimized by improved PSO. Computers and Electronics in Agriculture, 2016; 122: 94–102.
[14] Xu D, Du S F, van Willigenburg L G. Optimal control of Chinese solar greenhouse cultivation. Biosystems Engineering, 2018; 171: 205–219.
[15] Aschilean I, Rasoi G, Raboaca MS, Filote C, Culcer M. Design and concept of an energy system based on renewable sources for greenhouse sustainable agriculture. Energies, 2018; 11(5): 1201.
[16] Wang R, Wu H H, Dong B, Xu H, Li T L. The dynamic simulation of distribution regularity of solar radiation in the individual tomato plant inside the Chinese solar greenhouse. Advance Journal of Food Science and Technology, 2013; 12: 1543–1547.
[17] Zhang K, Yu J H, Ren Y. Research on the size optimization of photovoltaic panels and integrated application with Chinese solar greenhouses. Renewable Energy, 2022; 182: 536–551.
[18] Tong X J, Sun Z P, Sigrimis N, Li T L. Energy sustainability performance of a sliding cover solar greenhouse: solar energy capture aspects. Biosystems Engineering, 2018; 176: 88–102.
[19] Xu F, Shang C, Li H L, Guo W Z. Comparison of thermal and light performance in two typical Chinese solar greenhouses in Beijing. Int J Agric & Biol Eng, 2019; 12(1): 24–32.
[20] Zheng L, Zhang Q, Zheng K X, Zhao S M, Wang P Z, Cheng J Y, et al. Effects of diffuse light on microclimate of solar greenhouse, and photosynthesis and yield of greenhouse-grown tomatoes. Hortscience, 2020; 55(10): 1605–1613.
[21] Cao Y H, Sun Z F, Wu Y M, Li Y X. Research of auxiliary designing software GRLT in light transmissivity of greenhouse: The second part of serial studies on simulation of light environment of farming under structure. Transactions of the CSAE, 1992; 8(4): 69–77. (in Chinese)
[22] Chen Q Y. Numerical experiments on direct light transmission of single roof greenhouses. Transactions of the CSAE, 1993; 9(3): 96–101. (in Chinese)
[23] Xu H J, Cao Y F, Li Y R, Gao J, Jiang W J, Zou Z R. Establishment and application of solar radiation model in solar greenhouse. Transactions of the CSAE, 2019; 35(7): 160–169. (in Chinese)
[24] Ma C W, Zhao S M, Cheng J Y, Wang N, Jiang Y C, Wang S Y, et al. On establishing light environment model in Chinese solar greenhouse. Journal of Shenyang Agricultural University, 2013; 44(5): 513–517. (in Chinese)
[25] Zhang X D, Lv J, Xie J M, Yu J H, Zhang J, Tang C N, et al. Solar radiation allocation and spatial distribution in Chinese solar greenhouses: Model development and application. Energies, 2020; 13(5): 1108.
[26] Huang L, Deng L H, Li A G, Gao R, Zhang L H, Lei W J. Analytical model for solar radiation transmitting the curved transparent surface of solar greenhouse. Journal of Building Engineering, 2020; 32: 101785.
[27] Chen J T, Ma Y W, Pang Z Z. A mathematical model of global solar radiation to select the optimal shape and orientation of the greenhouses in southern China. Solar Energy, 2020; 205: 380–389.
[28] Pieters J G, Deltour J M. Modelling solar energy input in greenhouses. Solar Energy, 1999; 67(1-3): 119–130.
[29] Yan Q S, Zhao Q Z. Building thermal process. Beijing: China Construction Industry Press, 1996; 188p. (in Chinese)
[30] Zhou X H, Liang Y, Wang X M, Zhou L C. Comparison of saturation vapor pressure formulas. Journal of Liaoning Technical University, 2007(3): 331–333. (in Chinese)
[31] Li T L. Theory and Practice of Vegetable Cultivation in Sunlight Greenhouse. Beijing: China Agricultural Publishing House. 2013. (in Chinese)
[32] Zhang R, Liu Y C, Zhu D L, Ge M S. Establishment and application of daylighting efficiency model for the front roof covered with dust film in solar greenhouses. Transactions of the CSAE, 2021; 37(13): 190–199. (in Chinese)